

average energy of the charged particles would then be  $\bar{E}_p=0.35$  and  $\bar{E}_{\text{sec}}=0.30$  Bev, respectively. It has been pointed out<sup>6</sup> that for the two-center system the average longitudinal momentum  $\langle P_l \rangle$  of both the branches *A* and *B* in their own reference frames should be of the same order of magnitude as that of transverse momentum itself and we have found that for two branches of the primary event  $\langle P_l \rangle \approx 0.24$  and  $0.17$  while  $\langle P_l \rangle \approx 0.23$  and  $0.18$  for the forward and the backward cones, respectively. Similarly in the case of the secondary event the average longitudinal momentum is

approximately the same as that of the transverse momentum for each branch separately. The analysis of these events is consistent with the "two-fireball" model.

#### ACKNOWLEDGMENTS

We would like to express our deep appreciation for the hospitality of the late Professor Marcel Schein of the University of Chicago where this work started. We are also very grateful to Professor J. Nishimura for many stimulating discussions.

PHYSICAL REVIEW

VOLUME 125, NUMBER 2

JANUARY 15, 1962

### Spin and Parity of the $\omega$ Meson\*

M. L. STEVENSON, L. W. ALVAREZ, B. C. MAGLIĆ, AND A. H. ROSENFELD  
Lawrence Radiation Laboratory, University of California, Berkeley, California  
(Received September 15, 1961)

The spin and parity of the  $\omega$  meson have been determined to be  $1^-$  by a quantitative comparison of the density of points on the Dalitz plot with the predicted density of points. The simplest matrix element for the  $J=1^-$  meson (which predicts maximum density of points at the center of the Dalitz plot and zero density on the boundary) fits the data remarkably well. On the other hand, the simplest matrix elements for  $1^+$  and  $0^-$  mesons (both of which predict zero density at the center of the plot) do not fit at all. A quantitative treatment for higher  $J$  values has not been attempted. However, the simplest matrix elements for  $J=2^+$  and  $2^-$  also vanish at the center of the Dalitz plot, and are again inconsistent with the data.

**I**N a previous paper<sup>1,2</sup> we presented data suggesting a spin assignment  $J=1^-$  (vector meson).

The density of points on our Dalitz plot was depopulated near the boundary, and densely populated near the middle. This density was compared with the three possible simple matrix elements for  $J \leq 1$ . Their qualitative features are summarized in Table I, which is slightly more detailed than the version that we presented earlier. The meaning of the angular momenta **I** and **L** is as follows: The matrix element is analyzed in terms of a single pion plus a dipion. The pions of the dipion are assigned a momentum **q**, and an angular momentum **L** (in the dipion rest frame). Then another pair of variables, **p** and **l**, describe the remaining pion in the  $\omega$  rest frame.<sup>3</sup> A  $T=0$  state of three pions must

be antisymmetric in all pairs; hence all three of the competing matrix elements must vanish where any two pions "touch" in momentum space (i.e.,  $q=0$ ). This corresponds to regions *b*, *d*, and *f*, on the Dalitz plots in Fig. 1, *D* and *E*.

The three competing matrix elements have the following characteristics:

(a) The axial matrix element ( $1^-$  meson) involves cross products of momentum vectors and vanishes whenever all momenta are collinear. This occurs on the boundary of the Dalitz plot.

(b) The scalar matrix element ( $0^-$  meson) vanishes whenever two pions have the same energy, i.e., along the straight lines that divide the Dalitz plot.

(c) The vector matrix element ( $1^+$  meson) vanishes whenever all three pions have the same energy, i.e., at the center of the plot. In contrast to the scalar matrix element, it does not vanish at points *a*, *c*, and *e*, where  $|p|=0$  (the finite population here is contributed by the  $l=0$  partial wave). Values of  $p=1$  and  $2$  (units of  $m_\pi c$ ) are indicated in Fig. 1. *E*.

We concluded that the data suggest that  $\omega$  is a  $1^-$  meson. This paper presents quantitative support for

\* Work done under the auspices of the U. S. Atomic Energy Commission.

<sup>1</sup> B. C. Maglić, L. W. Alvarez, A. H. Rosenfeld, and M. L. Stevenson, Phys. Rev. Letters 7, 178 (1961).

<sup>2</sup> The collaborating groups of Johns Hopkins and Duke Universities have informed us of evidence for the  $\omega$  meson in the reaction  $\pi^+ + d \rightarrow p + p + \pi^+ + \pi^- + \pi^0$  at 1.23-Bev/c incident momentum. Further evidence for the  $\omega$  meson has been found by Xuong and Lynch in the reaction  $p + p \rightarrow 3\pi^+ + 3\pi^- + \pi^0$ . In their paper [N. H. Xuong and G. R. Lynch, Phys. Rev. Letters 7, 327 (1961)] they report  $M_\omega = 780$  and  $\Gamma/2 < 18$ .

<sup>3</sup> C. N. Yang (private communication) points out that the matrix elements of Table I must be formed of linear combinations of different values of  $L$  and  $l$ . Furthermore,  $L$  and  $l$  are meaningful only in the limit of nonrelativistic pions. In this limit, the following linear combinations are required:  $1^+$  meson,  $l=2$  and  $0$ ,  $L=1$ ;

$0^-$  meson,  $l=3$  and  $1$ ,  $L=3$  and  $1$ ; where  $l=1$ ,  $L=1$  is the minimum complexity necessary for the  $1^-$  meson. These additions are included in Table I.

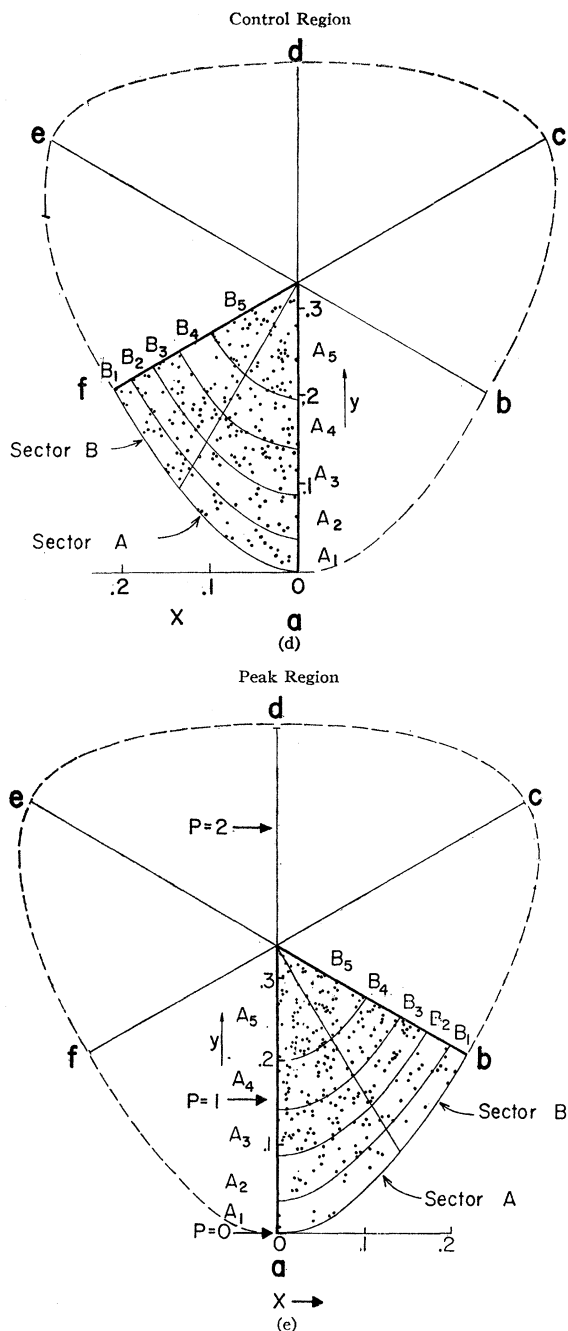
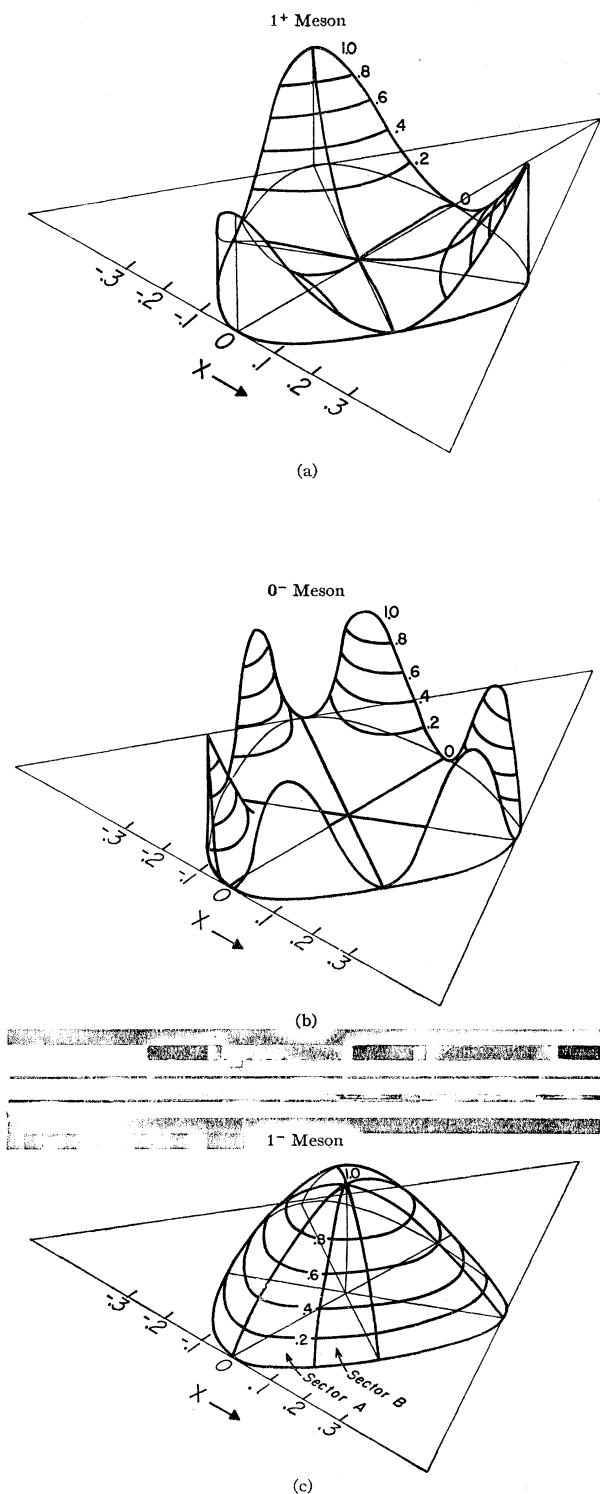


FIG. 1. (a), (b), and (c): Isometric drawings of the square of matrix elements for the  $1^+$ ,  $0^-$ , and  $1^-$  mesons expressed in terms of the normalized Dalitz variables  $x = (T_- - T_+)/\sqrt{3}Q$ , and  $y = T_0/Q$  ( $Q = T_+ + T_- + T_0 = M_3 - 3$ ). (d) and (e): Dalitz plots, folded six times. (d) displays 241 triplets in the control region and (e) displays 270 triplets in the peak region. The contour lines represent the projection of the contours of (c) ( $1^-$  meson).

that conclusion. Since our earlier Letter,<sup>1</sup> we have processed an additional 325 events of the type

$$\bar{p} + p \rightarrow \pi^+ + \pi^+ + \pi^- + \pi^- + \pi^0. \quad (1)$$

These have been added to our previous 800 events, and

the remainder of the discussion is based on all 1125 events.

The square of the matrix element,  $|\mathbf{A}|^2$ , has been calculated for the three possible mesons  $1^-$ ,  $0^-$ , and  $1^+$ . In terms of  $\mathbf{p}$ ,  $\mathbf{q}$  and  $\mu (= \hat{\mathbf{p}} \cdot \hat{\mathbf{q}})$ , the values of  $|\mathbf{A}|^2$  are:

TABLE I. Possible three-pion resonances with  $T=0$ ,  $J \leq 1$ .

Meson Type	$J$	$l$	$L$	Matrix element	
				Simple example	Vanishes at (see Fig. 1, $D$ and $E$ )
$V$	$1^-$	1	1	$(\mathbf{p}_0 \times \mathbf{p}_+) + (\mathbf{p}_+ \times \mathbf{p}_-) + (\mathbf{p}_- \times \mathbf{p}_0)$	Whole boundary
$PS$	$0^-$	1 and 3	1 and 3	$(E_- - E_0)(E_0 - E_+)(E_+ - E_-)$	Straight lines
$A$	$1^+$	0 and 2	1	$E_-(\mathbf{p}_0 - \mathbf{p}_+) + E_0(\mathbf{p}_+ - \mathbf{p}_-) + E_+(\mathbf{p}_- - \mathbf{p}_0)$	Center b, d, f.

$1^-$  meson,

$$|\mathbf{A}|^2 = 9p^2q^2(1-\mu^2), \quad (2)$$

$0^-$  meson,

$$|\mathbf{A}|^2 = \frac{\mu^2}{4} \left( \frac{p^2q^2}{q^2+1} \right) \left\{ [p^2+4(q^2+1)]^{\frac{3}{2}} - 2(p^2+1)^{\frac{3}{2}} \right. \\ \left. - \mu^2 \left( \frac{p^2q^2}{q^2+1} \right) \right\}, \quad (3)$$

$1^+$  meson,

$$|\mathbf{A}|^2 = \frac{q^2\mu^2}{q^2+1} \{ p^2 - 2(q^2+1) + (p^2+1)^{\frac{1}{2}} [p^2+4(q^2+1)]^{\frac{1}{2}} \}^2 \\ + q^2(1-\mu^2) \{ 2(p^2+1)^{\frac{1}{2}} - [p^2+4(q^2+1)]^{\frac{1}{2}} \}^2. \quad (4)$$

The relationship between  $p$ ,  $q$ , and  $M_3$ , the mass of the three-pion system is

$$p^2 = [(M_3+1)^2 - 4(q^2+1)][(M_3-1)^2 - 4(q^2+1)]/4M_3^2. \quad (5)$$

The boundary of the Dalitz plot corresponds to  $\mu^2=1$ . The straight lines that divide it correspond to  $\mu=0$ . From Eqs. (2)–(4), one sees that all the matrix elements vanish for  $q=0$ , as required by the  $T=0$  character of three pions. The other qualitative features are also evident.

Figures 1 A–C are isometric drawings of the square of the matrix elements for the  $1^+$ ,  $0^-$ , and  $1^-$  mesons, respectively. The coordinates in the plane are normalized Dalitz variables. The height above the plane is proportional to  $|\mathbf{A}|^2$ . The maximum height above the plane is chosen as unity and contours of equal values of  $|\mathbf{A}|^2$  are drawn at 0.2 intervals.

Before comparing the data with these  $|\mathbf{A}|^2$  distributions, both the data and  $|\mathbf{A}|^2$  can be folded six times about the lines of symmetry that divide the Dalitz plot. The points in Fig. 1D show the 241 pion triplets which fell in the control region ( $820 < M_3 < 900$  Mev); those in Fig. 1E are the 270 triplets which fall in the  $\omega$  peak region ( $740 < M_3 < 820$  Mev). The contours on Fig. 1,  $D$  and  $E$  are formed by projecting the contours of the  $1^-$  meson (Fig. 1C) onto the plane of the Dalitz plot. Since the  $|\mathbf{A}|^2$  for  $1^+$  and  $0^-$  mesons show considerable “azimuthal” variation, the folded area has been arbitrarily divided into two sectors  $A$  and  $B$ . The contours in turn divide each sector into five subsectors,  $A_1 \dots A_5$ ,  $B_1 \dots B_5$ .

The number of peak-region events per unit area

within  $A_1 \dots A_5$  and  $B_1 \dots B_5$  are displayed in the upper portions of Fig. 2,  $A$  and  $B$ , respectively. The normalized density of control-region events are displayed in the lower portions. The normalization accounts for the number of triplets that lie below the background curve in the peak region (169 triplets—see Fig. 3). Thus the density distribution of points in Fig. 1D is scaled by 169/241. A background subtraction is not meaningful because (a) we are uncertain of the difference in behavior of the  $T=0$  background in the peak region and in the control region and (b) we see no way of predicting what fractions of the  $T=0$  and  $T=1$  plus  $T=2$  states are present in the background.

The smooth curves for the three competing distributions are all normalized to the same number of events (in this case 270 for the peak region). The solid curve is the prediction of the  $1^-$  meson, the dashed curve for the  $1^+$  meson, and the broken curve for the  $0^-$  meson. In spite of the uncertainty of the background subtraction, the  $1^-$  meson is conclusively favored by the data.

We have tacitly assumed that the  $\omega$ -meson spin is  $J \leq 1$ . A quantitative treatment for higher  $J$  values has not been attempted. However, the simplest matrix elements for  $J=2^+$  and  $2^-$  also vanish at the center of

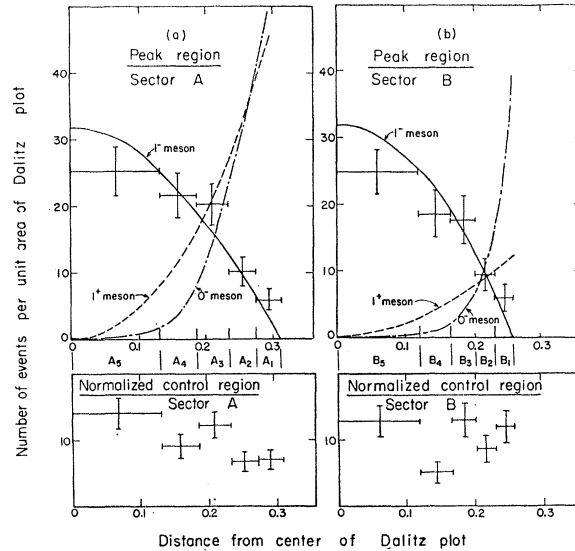


FIG. 2. (a) Density of points on the Dalitz plot for sectors  $A_1$  through  $A_5$ . (b) Density of points for sectors  $B_1$  through  $B_5$ . The sectors are defined by the contours for the  $1^-$  meson. The smooth curves are the probability distributions  $|\mathbf{A}|^2$  for the three competing matrix elements.

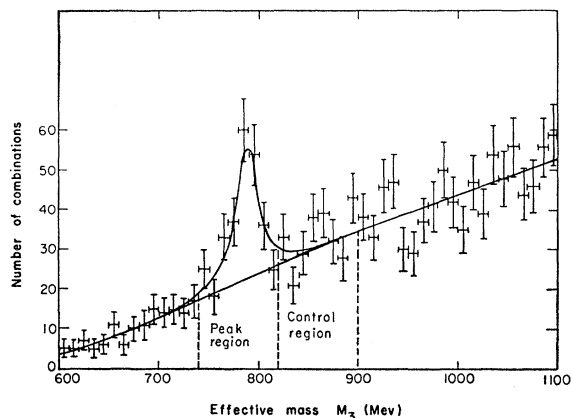


FIG. 3. Number of  $\pi^+\pi^-\pi^0$  triplets vs effective mass ( $M_3$ ) of the triplets for the reaction  $\bar{p} + p \rightarrow 2\pi^+ + 2\pi^- + \pi^0$ . The smooth curve drawn through the background has superposed upon it the experimental resolution function ( $\Gamma_{\text{resol}}/2 = 12$  Mev). The area under the resolution function is equal to the number of events above the background curve.

the Dalitz plot. This is certainly inconsistent with the data. We must conclude that the  $\omega$  is a vector meson,  $J=1^-$ .

Figure 3 shows a portion of the effective-mass distribution. A smooth curve has been drawn through the background and a curve (centered at  $M_3=787$  Mev) that represents our experimental resolution function ( $\Gamma_{\text{resol}}/2=12$  Mev) has been superposed upon it. The area under the resolution function is equal to the number of events that lie above the background curve in the vicinity of the peak. The data reasonably fit the resolution function. We conclude that the true half-

width  $\Gamma/2$  is consistent with zero, and is less than 12 Mev.

Finally, we have studied angular distributions and correlations in  $\omega$  meson breakup for the 270 triplets in the peak region. Within statistics, the  $\omega$  meson is produced isotropically. We define the production normal  $\mathbf{n}_1$  as  $\mathbf{p}(\text{beam}) \times \mathbf{p}(\omega)$ . The breakup normal  $\mathbf{n}_3$  (in the  $\omega$  rest frame) is the direction normal to its breakup plane. We find that  $\mathbf{n}_3$  is isotropic with respect to  $\mathbf{n}_1$ , to  $\mathbf{p}(\text{beam})$ , and to  $\mathbf{p}(\omega)$ . It is not correlated to the direction of breakup of the opposing dipion made in reaction (1).

We wish to point out that although our statistics are sufficiently good to allow a Dalitz-type analysis to be made, they are not such for the analysis of the angular distribution and correlations; a separate study must be made.

We again acknowledge the help that we received from those we mentioned in our earlier Letter. We regret that reference 9 of that Letter was garbled.<sup>4</sup> We also neglected to refer to the theoretical predictions of the  $\omega$  by Fujii<sup>5</sup> and Breit.<sup>6</sup> We are indebted to Professor J. Sakurai for pointing this out to us.

<sup>4</sup> The last part of reference 9 should have read: For previous evidence see: I. Derado, *Nuovo cimento* **15**, 853 (1960); E. Pickup, F. Ayer, and E. O. Salant, *Phys. Rev. Letters* **5**, 161 (1960); J. G. Rushbrooke and D. Radojčić, *ibid.* **5**, 567 (1960); J. Anderson, V. Bang, P. Burke, D. Carmony, and N. Schmitz, *ibid.* **6**, 365 (1961); A. R. Erwin, R. March, W. D. Walker, and E. West, *ibid.* **6**, 628 (1961); D. Stonehill, C. Baltay, H. Courant, W. Fickinger, E. C. Fowler, H. Kraybill, J. Sandweiss, J. Sanford, and H. Taft, *ibid.* **6**, 624 (1961).

<sup>5</sup> Y. Fujii, *Progr. Theoret. Phys. (Kyoto)* **21**, 232 (1959).

<sup>6</sup> G. Breit, *Proc. Natl. Acad. Sci. U. S. A.* **46**, 746 (1960); *Phys. Rev.* **120**, 287 (1960).

## $\pi^\pm - p$ Total Cross Sections in the Range 450 to 1650 Mev

THOMAS J. DEVLIN, BURTON J. MOYER, AND VICTOR PEREZ-MENDEZ  
Lawrence Radiation Laboratory, University of California, Berkeley, California

(Received August 17, 1961)

The total cross sections for positive and negative pions on hydrogen were measured at frequent intervals in the energy range from 450 to 1650 Mev. Six scintillation counters measured the transmission of pions at various solid angles, and the results were extrapolated to zero solid angle. The two peaks previously discovered in the  $\pi^- - p$  cross section were observed to be centered at  $600 \pm 15$  Mev and  $900 \pm 15$  Mev. A broad maximum was observed in the  $\pi^+ - p$  cross section at approximately 1350 Mev. A "shoulder" at approximately 800 Mev, in a region where the  $\pi^+ - p$  cross section is rapidly rising, supports speculation that there is a resonant state at this energy. Except for a small, unresolved difference in absolute values in the  $\pi^\pm - p$  case, these data agree with those obtained by Brisson *et al.* at Saclay.

### I. INTRODUCTION

PRIOR to 1955, little work was done in the investigation of pion-proton scattering above 300 Mev.<sup>1</sup> Since that time, experiments have indicated that there

<sup>1</sup> H. Bethe and F. de Hoffmann, *Mesons and Fields*, (Row, Peterson and Company, Evanston, Illinois, 1955), Vol. 2. This reference contains a summary of work done before 1955.

is important structure in the graph of total cross section vs energy from 300 Mev to 2 Bev. Investigations at the Brookhaven Cosmotron<sup>2</sup> indicated the presence of broad maxima in the  $\pi^- - p$  cross section near 900 Mev, and in the  $\pi^+ - p$  cross section near 1.4 Bev. A group

<sup>2</sup> R. Cool, O. Piccioni, and D. Clark, *Phys. Rev.* **103**, 1082 (1956).